Chemical Engineering Science 64 (2009) 3510 – 3515

Contents lists available at ScienceDirect

Chemical Engineering Science

journal homepage: www.elsevier.com/locate/ces

The effect of CO_2 and salinity on olivine dissolution kinetics at 120 °C

Valentina Prigiobbe[a], Giulia Costa[b], Renato Baciocchi[b], Markus Hänchen[a,1], Marco Mazzotti[a,*]

[a]Institute of Process Engineering, ETH Zurich, Zurich, Switzerland
[b]Department of Civil Engineering, University of Rome "Tor Vergata", Rome, Italy

ARTICLE INFO

Article history:
Received 23 December 2008
Received in revised form 23 April 2009
Accepted 27 April 2009
Available online 5 May 2009

Keywords:
Carbon dioxide capture and storage (CCS)
Mineral carbonation
Dissolution
Kinetics
Mathematical modeling
Population balance equation

ABSTRACT

This paper reports the results of an experimental study on the dissolution kinetics of olivine ($Mg_{1.82}Fe_{0.18}SiO_4$) at operating conditions relevant to the mineral carbonation process for the permanent storage of CO_2. In particular, we investigated the effects of CO_2 fugacity (f_{CO_2}) and of salinity on the kinetics of olivine dissolution, which is assumed to be the rate-limiting step of the overall carbonation process. Dissolution experiments were carried out at 120 °C in a stirred flow-through reactor. Different pH values (between 3 and 8) and solution compositions were investigated by varying f_{CO_2} and by dosing LiOH (for pH control), NaCl, and $NaNO_3$. The specific dissolution rate values, r, were estimated from the experimental data using a population balance equation (PBE) model coupled with a mass balance equation. The logarithms of the obtained r values were regressed with a linear model as a function of pH and compared to the model reported earlier [Hänchen, M., Krevor, S., Mazzotti, M., Lackner, K.S., 2007. Validation of a population balance model for olivine dissolution. Chem. Eng. Sci. 62, 6412–6422] for experiments with neither CO_2 nor salts. Our results confirm that, at a given temperature, olivine dissolution kinetics depends on pH only, and that f_{CO_2} and the concentrations of NaCl and $NaNO_3$ affect it through their effect on pH.

1. Introduction

Aqueous mineral carbonation is a technology that is being studied and developed in the framework of the carbon dioxide capture and storage (CCS) systems (IPCC, 2005). It aims at binding CO_2 into stable carbonates, using metal oxides via a high-pressure and high-temperature *ex situ* process, which mimics natural rock weathering. For a large scale implementation of this process, the most suitable sources of metal oxides are magnesium silicate minerals, such as olivine and serpentine, due to their large worldwide availability (e.g. in ophiolite belts) (Goff et al., 2000).

Aqueous mineral carbonation of olivine involves CO_2 dissolution in water, the dissolution of the silicate minerals, and the precipitation of Mg–carbonates. In particular, the dissolution of the silicate minerals is considered to be the rate-limiting step of the entire aqueous mineral carbonation process. In the case of the dissolution of forsterite, the magnesium end-member of olivine, the chemical reaction in a CO_2-free solution is

$$Mg_2SiO_{4(s)} + 4H_2O \rightleftharpoons 2Mg^{2+}_{(aq)} + H_4SiO_{4(aq)} + 4OH^-_{(aq)}. \quad (1)$$

This reaction has been extensively studied at ambient pressure and temperature and its kinetics has been found to depend primarily on pH. Two different mechanisms for olivine dissolution have been postulated at 25 °C, corresponding to a pH-dependence for pH < 8, and to no pH-dependence for higher values (Wogelius and Walther, 1991; Pokrovsky and Schott, 2000; Rosso and Rimstidt, 2000). The first mechanism is governed by the adsorption of one H^+ ion onto two olivine cells leading to a preferential release of magnesium over silicon and to the formation of a thin Mg-depleted, and Si-rich (altered) layer. At higher pH values, the dissolution is controlled by the formation of $Mg(OH)^+_2$ complexes and exhibits a preferential release of silicon into solution, thus creating a Si-depleted and hence Mg-rich surface layer. Recently, we have studied olivine dissolution at temperatures between 90 and 150 °C and at pH values between 2 and 12.5 (tuned using HCl and LiOH), and we have observed the same behavior (Hänchen et al., 2006), and hence we proposed the same mechanism. In particular, the specific dissolution rate, r, depends on pH in the pH range from 2 to 8.5, and it is given by the following equation (that corresponds to a linear dependence of the logarithm of r on pH at a given temperature):

$$r = a^n_{H^+} A\, e^{-E_a/RT}, \quad (2)$$

where r is the specific dissolution rate (mol cm^{-2} s^{-1}), T is the temperature (K), R is the gas constant (8.3145×10^{-3} kJ K^{-1} mol^{-1}), a_{H^+} is the hydrogen ion activity (dimensionless), and A is a pre-exponential

* Corresponding author. Tel.: +41 44 6322456; fax: +41 44 6321141.
E-mail address: marco.mazzotti@ipe.mavt.ethz.ch (M. Mazzotti).
[1] Present address: Paul Scherrer Institute, Villigen PSI, Switzerland.

0009-2509/$ - see front matter © 2009 Elsevier Ltd. All rights reserved.
doi:10.1016/j.ces.2009.04.035

factor ($mol\,cm^{-2}\,s^{-1}$). In the above mentioned study (Hänchen et al., 2006) the parameters A, E_a (activation energy), and n (reaction order for H^+) were estimated by fitting all the experiments to Eq. (2), thus resulting in the following values: $A = 0.0854\,mol\,cm^{-2}\,s^{-1}$, $E_a = 52.9\,kJ\,mol^{-1}$, and $n = 0.46$. Moreover, to assess the influence of CO_2 on olivine dissolution, in the same work a few experiments were also carried out at 120 °C under a CO_2 partial pressure (from 15 to 180 bar) and in a pH range between 3 and 6 (adjusted by LiOH addition) (Hänchen et al., 2006). The measured dissolution rates were the same as, or slightly higher than, those without CO_2 up to a pH value of 5, and markedly lower beyond this value. Although earlier studies have reported and justified such dissolution inhibition (Wogelius and Walther, 1991; Pokrovsky and Schott, 2000), others have questioned such a conclusion (Golubev et al., 2005). There is, however, agreement about the importance of the formation of Mg–carbonate complexes on the olivine surface in determining the dissolution behavior. It is worth noting that the pH effect on silicate dissolution can in principle be exploited to control the mineral carbonation process, namely by dissolving silicates at low pH and by precipitating carbonates at high pH, i.e. through a so-called pH-swing process (Park et al., 2004).

Inorganic salts such as NaCl, $NaHCO_3$, and $KHCO_3$ have been used in different works to enhance the carbonation of silicates (Geerlings et al., 2002; O'Connor et al., 2005; McKelvy et al., 2005). However, in a thorough study of forsterite CO_2-free dissolution at 25 °C in a pH range from 1 to 4, it has been shown that the dissolution rate was not affected by the presence of the inorganic salts KNO_3, $Mg(NO_3)_2$, Na_2SO_4, and $MgSO_4$ at an ionic strength of up to $12\,mol\,kg^{-1}$ (Olsen, 2007). Nevertheless, specific studies regarding the dissolution kinetics of Mg-silicates at high CO_2 fugacity, salinity, and temperature, the operating conditions typically reported for the mineral carbonation process (O'Connor et al., 2005), are still missing. Hence, the effects of CO_2 and salinity on olivine dissolution kinetics are not clear enough, both qualitatively and quantitatively, at the conditions of interest for mineral carbonation. Thus, with this work we aimed at achieving a deeper understanding of these effects on olivine dissolution kinetics in order to be able to optimize the mineral carbonation process. Olivine dissolution was studied at 120 °C in a H_2O–CO_2–LiOH–NaCl/$NaNO_3$ system, for different values of CO_2 fugacity (in the range 0.4–123 bar), of pH (2–8), and of salinity (salt concentration up to $2.5\,mol\,kg^{-1}$). For each experiment, the values of r were estimated by fitting the experimental data (olivine concentration vs. time) with a population balance equation (PBE) model coupled with a mass balance equation (Hänchen et al., 2007). Finally, the obtained values of r were regressed using the model reported in Eq. (2).

2. Materials and methods

The dissolution kinetics of natural San Carlos gem-quality olivine grains ($Mg_{1.82}Fe_{0.18}SiO_4$), with a particle size between 90 and 180 μm and a specific surface of $797 \pm 55\,cm^2\,g^{-1}$, was studied in a LiOH–CO_2 aqueous system. Selected experiments were also carried out in NaCl/$NaNO_3$–LiOH–CO_2 aqueous solutions. Small amounts of LiOH were added to the solution in order to achieve pH values higher than 4 in the presence of CO_2. This hydroxide was chosen since Li^+ concentrations of the solution could be accurately monitored online, as described below. A flow-through high-pressure high-temperature titanium reactor, as described in Hänchen et al. (2006), was used for all experiments. All runs were performed at a temperature of 120 °C, with a liquid volume of 170 ml and a gas headspace of 130 ml. Carbon dioxide 99.995% vol.-purity (PanGas, Werk Dagmersellen, Switzerland), fed to the reactor from a high-pressure buffer tank and via a front-pressure regulator, was used to pressurize the solution at specific values, ranging from 2 to 100 bar. The gas was fed to the solution through the stirrer to facilitate the achievement of gas–liquid equilibrium. The stirrer was operated at 700 rpm to avoid mixing limitations and particle sedimentation.

For the entire duration of each experiment, the feed solution was purged with N_2 99.999% vol.-purity (PanGas, Werk Dagmersellen, Switzerland), fed directly from a gas cylinder. Such a solution, consisting of ultrapure water only or of ultrapure water with electrolytes, i.e. LiOH, NaCl, and $NaNO_3$, was introduced into the reactor at a constant flow rate of either 2 or $5\,ml\,min^{-1}$, after being pre-heated up to 90 °C with a heat exchanger, in order to minimize the temperature drop at the entrance of the reactor. A second HPLC pump was used to withdraw liquid at exactly the same flow rate as the inlet pump, in order to maintain a constant liquid level in the reactor. Before passing through the second pump, the outlet stream was cooled down to ambient temperature by a copper-tubular heat exchanger, then its flow rate was measured with a flow meter and finally it was depressurized to ambient pressure by using a hydraulic disconnection. For each experiment, the reactor was initially filled with a known amount of olivine, closed, and flushed with CO_2 to purge O_2 from it. Then a known amount of solution was pumped into the vessel and heated up to 120 °C. Once the system stabilized, the reactor was pressurized and kept at these conditions for the entire run. The Mg^{2+} and Li^+ concentrations in the outlet solution were measured online by means of an ion chromatograph (CS12A column, Dionex). Solution samples were taken with a fraction collector at regular intervals and their silicon concentration was measured with a spectrophotometer using the Molybdate Blue method (Grasshoff and Anderson, 1999; ICRAM, 2001). The standards for the Mg^{2+} and Si^{4+} measurements were prepared with the feed solution to take into account the effects of salinity on the analysis. In order to estimate the pH, the geochemical software package EQ3/6 v8.0 (Wolery and Jarek, 2003) was used to model the composition of the solution, assuming that the time scale for achieving equilibrium was smaller than the residence time (30–90 min). A database employing Pitzer equations to estimate the activity coefficients of the aqueous species at high ionic strengths was used. Based on the measured temperature and pressure, the CO_2 fugacity was calculated by using a noniterative procedure developed by Spycher et al. (2003), based on the Redlich–Kwong equation of state for the CO_2–H_2O mixture. The value of f_{CO_2} together with the temperature and Mg^{2+} and Si^{4+} concentrations was used to calculate the actual pH value using EQ3/6.

3. Modeling

Following Hänchen et al. (2007), the dissolution of olivine was modeled by a 1-D population balance equation model, assuming constant particle shape. This equation together with a flow-through reactor model allows the description of the temporal evolution of olivine particles. The governing equations are given by

$$\frac{\partial f}{\partial t} - D\frac{\partial f}{\partial L} = 0, \tag{3}$$

$$V\frac{dc}{dt} + Qc = -\frac{dm}{dt}, \tag{4}$$

where f is the unscaled particle size distribution number density (m^{-1}); D is the dissolution rate ($m\,s^{-1}$); m is the total mass of particles (moles of olivine); V is the volume of the suspension (m^3); Q is the flow rate through the reactor ($m^3\,s^{-1}$); c is the concentration of olivine in solution ($mol\,m^{-3}$), and L is the characteristic length of a particle (m).

The model consisting of Eqs. (3) and (4) must be solved numerically for a given initial mass of olivine and a given initial particle size distribution, thus yielding the time evolution of the olivine concentration c in solution. To this aim, we used a combination of the method of characteristics and of the method of moments

Table 1
Olivine dissolution at 120 °C: operating conditions and experimental results.

pH	f_{CO_2} (bar)	Li^+(mol kg^{-1})	Salt (mol kg^{-1})	Q (ml min^{-1})	V (ml)	m_0 (mg)	Duration (h)	r (mol cm^{-2} s^{-1}) $\times 10^{10}$	Exp. no.
2.01	–	0	0	10.37	160	55	10.0	10.3	28
2.02	–	0	0	10.37	160	59	9.5	11.2	27
2.02	–	0	0	10.37	160	68	7.0	15.0	34
4.24	–	0	0	10.3	180	149	3.0	0.95	37
5.13	–	0	0	4.95	168.4	203	5.0	0.41	36
6.31	–	0	0	10.34	163	401	4.0	0.12	29
6.49	–	0	0	10.37	163	401	4.0	0.13	30
8.33	–	0	0	5.054	160	1002	10.0	0.0168	32
3.35	103.8	0	0	1.9	116.47	6.6	3	7.43	55
3.4	80.5	0	0	1.9	163.7	6.4	7	6.65	54
3.43	102.9	0	0	1.9	130.87	4.9	6	5.00	114
3.44	80.5	0	0	1.9	177.86	11.3	7	4.50	92
3.45	123.2	0	0	1.9	203.54	6.1	6	8.50	56
3.83	19.8	0	0	2	158.37	5.2	6	4.35	115
3.87	80.6	0	0	4.9	203.25	27.7	6	2.90	64
3.89	80.5	0	0	5.1	184.05	30.6	7	2.25	94
4.22	79.6	0.004	0	1.9	199.97	13.3	7	1.67	60
4.5	14.3	0.0013	0	5	168.92	13.9	6	1.00	116
4.75	14.3	0.0024	0	5	172.57	34.1	7	0.70	117
5.08	13.8	0.0053	0	5	175.05	68.8	7	0.60	66
5.08	13.5	0.0053	0	5.1	166.67	60.8	7	0.717	96
5.42	13.7	0.012	0	5.1	171.73	123.4	6	0.60	118
5.69	12.6	0.026	0	5.1	154.95	187	12	0.20	68
5.71	13.8	0.026	0	5.1	169.38	186.8	6	0.377	97
5.96	14.7	0.053	0	5.1	162.16	62	6	0.110	95
6.04	13.5	0.06	0	5.1	138.77	211.6	5	0.195	98
6.21	13.5	0.096	0	4.8	170.85	101	9	0.148	106
6.34	13.4	0.14	0	5.1	173.93	106.8	7	0.155	112
6.4	15.1	0.19	0	5.1	174.01	229.3	2	0.0695	99
6.45	13.5	0.19	0	5.1	180.10	302	7	0.101	100
6.59	5.6	0.096	0	5.1	192.57	103	9	0.058	109
6.68	4.5	0.096	0	5.1	174.84	101.5	4	0.115	107
6.82	4.5	0.14	0	5.1	184.05	108.9	8	0.118	108
6.84	4.3	0.14	0	5.1	180.56	109.1	9	0.0709	113
7.1	1.8	0.096	0	5.1	191.98	104.8	4	0.0513	110
7.81	0.4	0.14	0	5	201.02	105.6	5	0.020	111
3.21	80.6	0	1*	5	181.03	12	6	8.64	63
3.45	79.6	0	2.5*	5	213.17	23	7	2.28	70
3.64	80.6	0	0.1*	4.4	198.81	100.2	3	3.67	62
4.08	13.7	0.0013	2*	5.4	165.25	13.4	6	5.37	122
4.1	13.7	0.0013	1**	5.3	171.15	13.2	7	1.67	120
4.14	13.7	0.0013	1*	5.2	169.18	13.1	6	3.42	119
4.31	13.7	0.0024	2*	5.4	208.17	51.3	7	0.743	131
4.64	13.7	0.0024	0.1*	5	180.37	47.5	5	0.878	130
4.73	13.7	0.0024	0.01*	5	173.34	54.9	5	0.90	129
4.8	4.1	0.0024	2*	5.3	185.85	47.3	7	0.878	125
4.85	4.8	0.0024	1*	5.3	179.65	43.8	7	0.830	121
4.9	4.1	0.0024	1**	5.3	177.36	52.8	6	0.634	127
5.4	14.3	0.026	1*	5.1	189.35	47.4	6	1.15	128
5.41	13.7	0.026	1*	5.3	175.33	49.2	5	0.107	123
5.65	14.3	0.06	2*	5.5	223.86	48.5	6	0.228	135
5.74	14.3	0.06	1*	5.2	173.4	51.9	5	0.319	133
5.76	13.7	0.06	1*	5.2	174.92	45.5	6	0.454	134
5.96	13.7	0.096	1*	5.9	176.73	47.4	4	0.0917	124

Symbols indicate type of salt, * NaCl and ** $NaNO_3$.

(Hänchen et al., 2007) (note, however, that in that work, due to a typo, in Eq. (23) there is a factor t before the integral that should not be there). By fitting such evolution to the experimental concentrations of Mg^{2+} (c_{Mg}) and Si^{4+} (c_{Si}), expressed as olivine equivalents (c), that in a perfect stoichiometric dissolution process, is given by

$$c = c_{Si} = \frac{c_{Mg}}{1.82}, \tag{5}$$

the value of the dissolution rate D corresponding to the chosen operating conditions (pH, CO_2 fugacity, salinity) was estimated. Following the procedure explained earlier (Hänchen et al., 2007) a value of the specific dissolution rate r was calculated from the fitted value of D using information about the initial particle size distribution and the BET surface area of the initial particles.

4. Results and discussion

Specific data regarding olivine dissolution experiments carried out at 120 °C are reported in Table 1. In particular, for each experiment, the applied operating conditions, i.e. CO_2 fugacity (f_{CO_2}), LiOH (Li^+) and salt (either NaCl or $NaNO_3$) concentrations, flow rate (Q), suspension volume (V), initial olivine mass (m_0), and duration of the experiment are listed, together with the resulting specific dissolution rate (r), and the calculated pH. Two sets of experiments are shown:

- Experiments 27–37 (reported also in Hänchen et al., 2006), carried out with neither CO_2 nor salt, in which the pH was set by adding HCl or LiOH.

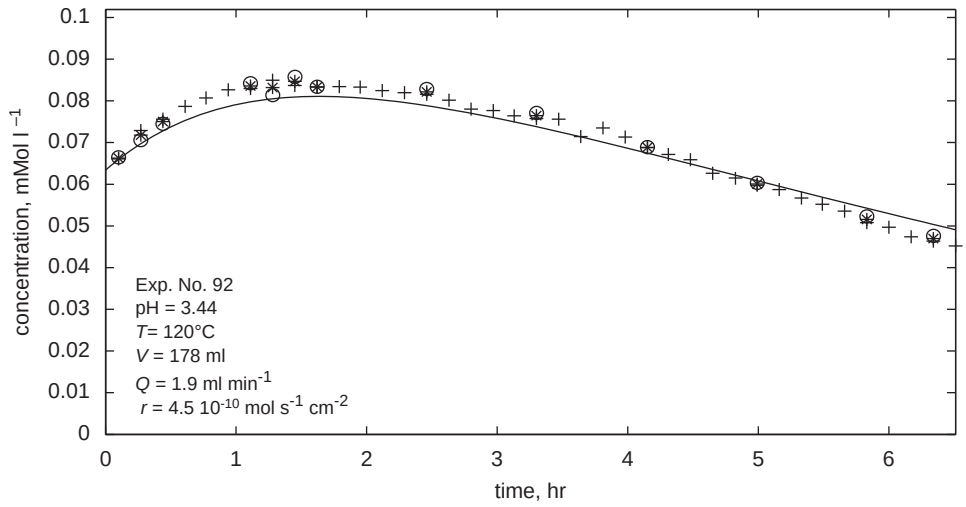

Fig. 1. Ion concentration over time during a fast dissolution experiment, Exp. no. 92. Symbols: (+) Mg^{2+} concentration, (○) Si^{4+} concentration, (∗) arithmetic average, and (–) model.

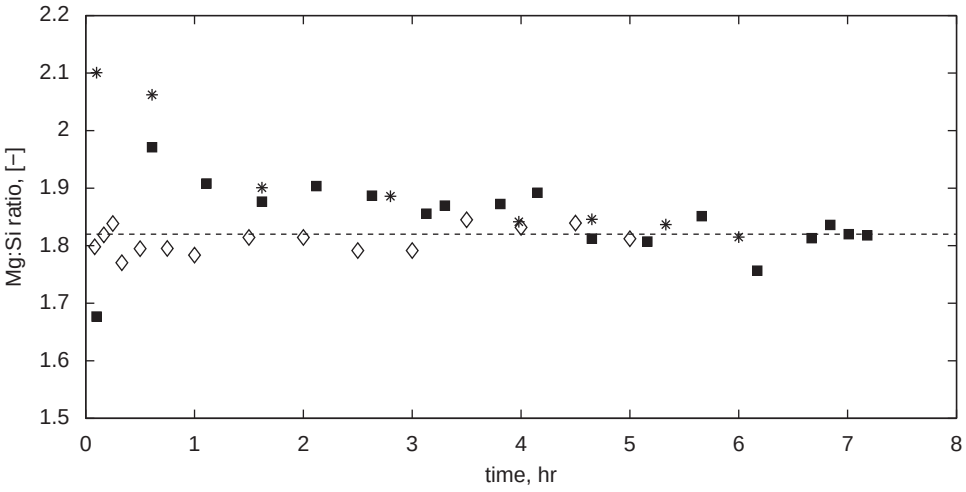

Fig. 2. Mg:Si ratio over time. Symbols: (⋄) experiment without CO_2 at pH 5.14 (no. 36, in Hänchen et al., 2006); (■) experiment with CO_2, but without salts at pH 4.22 (no. 60, in Table 1); (∗) experiment with CO_2 and 1 mol kg^{-1} NaCl at pH 4.14 (no. 119, in Table 1).

- Experiments 54–135, performed under a CO_2 atmosphere with or without salt addition, all of which previously unpublished data, except for experiments 54–68 already reported by Hänchen et al. (2006).

As an example, in Fig. 1 Exp. no. 92 (at pH = 3.44, corresponding to fast dissolution) is analyzed in more detail. In particular, the measured Mg^{2+} and Si^{4+} concentrations, expressed in olivine equivalents according to Eq. (5), are plotted over time, together with their arithmetic average. These experimental data are compared with the simulation results, obtained by solving Eqs. (3) and (4), numerically. The specific dissolution rate r, reported in the figure legend, was obtained by least-squared minimization of the residuals between the experimental data and the model results. In this case, the agreement is rather satisfactory, as in all the other experiments. In Fig. 1, the Mg^{2+} and Si^{4+} concentrations vary in time according to the dissolution dynamics, but remain always in their stoichiometric ratio. This was not always the case, as illustrated in Fig. 2, where the time evolution of the ratio of the two concentrations is plotted in the case of the Exp. nos. 36, 60, and 119. The behavior observed in this figure is indeed general, thus indicating that after an initial transient phase, the Mg^{2+} to Si^{4+} concentration ratio stabilized to its stoichiometric value. For modeling and regression purposes and to reduce the variability, the arithmetic average of the two concentrations expressed in olivine equivalents was used (Eq. (5)).

For all the experiments reported in Table 1, the logarithm of the value of r, estimated using the method described in Section 2, is plotted as a function of the calculated pH value in Fig. 3. In this figure, we plot also the values obtained in eight experiments without CO_2, where HCl was used to acidify the solution, that were reported and analyzed in our previous work (Hänchen et al., 2007). Experiments carried out with and without CO_2, with and without salt addition, can be distinguished by the different symbols.

The main conclusion that can be drawn by analyzing these results is that the change in the dissolution rate could be accounted for by the change in solution pH only. Varying the CO_2 fugacity, or the LiOH or HCl concentration, or the salinity, produced a change in the pH value, which in turn led to a change in r, but there was no evidence of a direct and independent effect of these parameters on the dissolution rate. Therefore, all experimental data in Fig. 3 were

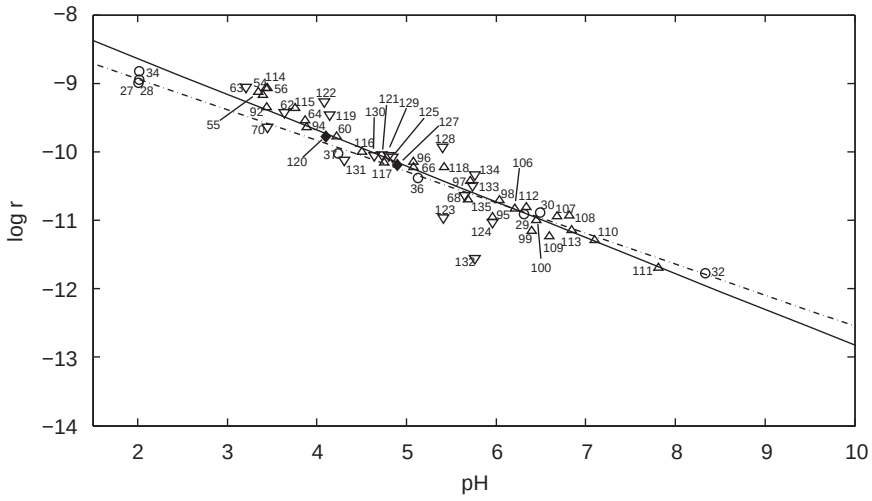

Fig. 3. Logarithm of r values plotted over pH for each run at 120 °C and linear model described in Eq. (2). Namely, (○) experiments without CO_2; (△) experiments with CO_2, with or without LiOH; (▽) experiments with CO_2 and NaCl; (♦) experiments with CO_2 and $NaNO_3$; (—) Eq. (6) with $n = 0.523$ and $B = 7.59$ (this work); (-·-) Eq. (6) with $n = 0.46$ and $B = 8.05$ (Hänchen et al., 2007).

regressed using a single equation, namely the following linearized form of Eq. (2):

$$\log r = -n\mathrm{pH} + B \tag{6}$$

with r in mol $cm^{-2}\,s^{-1}$, $\mathrm{pH} = -\log a_{H^+}$, $n = 0.523 \pm 0.047$, and $B = -7.59 \pm 0.24$, defined as the logarithm of $A\,e^{-E_a/RT}$, based on a 95% confidence interval (this corresponds to $A = 0.264\,\mathrm{mol\,cm^{-2}\,s^{-1}}$ in Eq. (2)) with a regression coefficient $R^2 = 0.91$. The corresponding straight line is plotted as a solid line in the same figure, where it can be compared with the same regression determined earlier (dash-dotted line) and based on a much smaller set of CO_2-free dissolution experiments, where $n = 0.46 \pm 0.03$, $B = -8.05 \pm 0.13$, and $R^2 = 0.98$ (Hänchen et al., 2006, 2007). It is worth noting that although the regression coefficient was higher in the earlier work because the regression was based on a smaller number of more homogeneous data (neither CO_2 nor salt present), the value of the reaction order n obtained in this study was closer to the theoretical value of 0.5. The two regression lines were anyhow in good agreement, considering also the experimental variability. The only noticeable difference was a slight dissolution enhancement at low pH values in the new regression. As to the effect of CO_2, which was considered to be detrimental at pH values larger than 5 in our earlier work (Hänchen et al., 2006), we believe that the large amount of consistent experimental evidence reported in this work demonstrates that such an effect was an artifact. We presume the inconsistency of the earlier measurements (Hänchen et al., 2006) was due to the very small amount of dissolved olivine on which the estimated values of the dissolution rate were based.

5. Conclusion

The conclusion of this comprehensive experimental work is simple but rather significant. The specific dissolution rate of olivine at a given temperature in the pH range between 2 and 8 depends on pH only. The effects of CO_2 fugacity, LiOH, HCl, salt concentrations, and combinations thereof are important inasmuch as they affect the pH, but not directly and independently. There is no inhibition effect of the presence of CO_2 on olivine dissolution at pH higher than 5 as previously reported, which is important because these are the conditions where carbonate precipitation is favored. Our investigation was carried out at 120 °C, but we would argue that our conclusions are general and could be applied to any temperature in the range between 25 and 150 °C, where several studies by our group and others have shown that the dissolution mechanism is the same. We believe that this is an important finding towards the design and optimization of an effective mineral carbonation process.

Acknowledgments

Financial support from the Foundation Claude & Giuliana, Basel, Switzerland, and Schweizerische Nationalfonds (SNF) are gratefully acknowledged.

References

Geerlings, J.J.C., Mesters, C.M.A.M., Oosterbeek, H., 2002. Process for mineral carbonation with carbon dioxide. Patent number WO02085788.

Goff, F., Guthrie, G.D., Lipin, B., Fite, M., Chipera, S.J., Counce, D., Kluk, E., Ziock, H.J., 2000. Evaluation of ultramafic deposits in the eastern United States and Puerto Rico as sources of magnesium for carbon dioxide sequestration. Technical Report LA-13694-MS, Los Alamos National Laboratory.

Golubev, S.V., Pokrovsky, O.S., Schott, J., 2005. Experimental determination of the effect of dissolved CO_2 on the dissolution kinetics of Mg and Ca silicates at 25 °C. Chem. Geol. 217, 227–238.

Grasshoff, K., Anderson, L.G., 1999. Methods of Seawater Analysis. third ed. Wiley-VCH, Weinheim.

Hänchen, M., Prigiobbe, V., Storti, G., Seward, T.M., Mazzotti, M., 2006. Dissolution kinetics of fosteritic olivine at 90–150 °C including effects of the presence of CO_2. Geochim. Cosmochim. Acta 70 (17), 4403–4416.

Hänchen, M., Krevor, S., Mazzotti, M., Lackner, K.S., 2007. Validation of a population balance model for olivine dissolution. Chem. Eng. Sci. 62, 6412–6422.

ICRAM, 2001. Ministero dell'Ambiente e della Tutela del Territorio-Servizio Difesa Mare. ICRAM, Metodiche Analitiche di Riferimento, p. 192.

IPCC, 2005. In: Metz, B., Davidson, O., de Coninck, H.C., Loos, M., Meyer, L.A. (Eds.), IPCC Special Report on Carbon Dioxide Capture and Storage. Cambridge University Press, Cambridge, UK, New York, NY, USA, 442pp.

McKelvy, M.J., Chizmeshya, A.V.G., Squires, K., Carpenter, R.W., Béarat, H., 2005. A novel approach to mineral carbonation: enhancing carbonation while avoiding mineral pretreatment process cost. DOE/DE-FG26-04NT42124, Arizona State University.

O'Connor, W.K., Dahlin, D.C., Rush, G.E., Dahlin, C.L., Collins, W.K., 2002. Carbon dioxide sequestration by direct mineral carbonation: process mineralogy of feed and products. Miner. Metall. Process. 19 (2), 95–101.

Olsen, A.A., 2007. Forsterite dissolution kinetics: applications and implications for chemical weathering. Ph.D. Thesis, Blacksburg, Virginia. Available at ⟨http://scholar.lib.vt.edu/theses/available/etd-07052007-135551/unrestricted/olsen.pdf⟩.

Park, A.-H.A., Fan, L.-S., 2004. CO_2 mineral sequestration: physically activated dissolution of serpentine and pH swing process. Chem. Eng. Sci. 59, 5241–5247.

Pokrovsky, O.S., Schott, J., 2000. Kinetics and mechanism of forsterite dissolution at 25 °C and pH from 1 to 12. Geochim. Cosmochim. Acta 64 (19), 3313–3325.
Rosso, J.J., Rimstidt, J.D., 2000. A high resolution study of forsterite dissolution rates. Geochim. Cosmochim. Acta 64, 797–811.
Spycher, N., Pruess, K., Ennis-King, J., 2003. CO_2–H_2O mixtures in the geological sequestration of CO_2. I. Assessment and calculation of mutual solubilities from 12 to 100 °C and up to 600 bar. Geochim. Cosmochim. Acta 67, 3015–3031.
Wogelius, R.A., Walter, J.V., 1991. Olivine dissolution at 25 °C: effects of pH, CO_2, and organic acids. Geochim. Cosmochim. Acta 55, 943–954.
Wolery, T.W., Jarek, R.L., 2003. Software user's manual. EQ3/6, Version 8.0, US Department of Energy Report, Sandia National Laboratories.